

Design and synthesis of a series of novel pyrazolopyridines as HIF-1 α prolyl hydroxylase inhibitors

Namal C. Warshakoon,* Shengde Wu, Angelique Boyer, Richard Kawamoto, Sean Renock, Kevin Xu, Matthew Pokross, Artem G. Evdokimov, Songtao Zhou, Carol Winter, Richard Walter and Marlene Mekel

Procter & Gamble Pharmaceuticals Inc, 8700 Mason-Montgomery road, Mason, OH 45040, USA

Received 12 June 2006; revised 26 July 2006; accepted 1 August 2006

Abstract—Recently resolved X-ray crystal structure of HIF-1 α prolyl hydroxylase was used to design and develop a novel series of pyrazolopyridines as potent HIF-1 α prolyl hydroxylase inhibitors. The activity of these compounds was determined in a human EGLN-1 assay. Structure-based design aided in optimizing the potency of the initial lead (**2**, IC₅₀ of 11 μ M) to a potent (**11**, 190 nM) EGLN-1 inhibitor. Several of these analogs were potent VEGF inducers in a cell-based assay. These pyrazolopyridines were also effective in stabilizing HIF-1 α .
© 2006 Elsevier Ltd. All rights reserved.

Hypoxia inducible factor (HIF) is a transcriptional complex that plays a key role in mammalian oxygen homeostasis and regulates a host of hypoxic response genes that regulate angiogenic, glycolytic, and erythropoietic processes.^{1–3} The subunit components, HIF-1 α and HIF-1 β (ARNT) are constitutively expressed and regulation is achieved by the selective destruction of HIF-1 α . HIF-1 α is a major regulatory point of cellular response to hypoxia (decreasing partial pressure of oxygen).

In the presence of oxygen, a family of non-heme iron containing prolyl hydroxylases (EGLN-1, EGLN-2, and EGLN-3) effects post-translational modification of HIF-1 α by hydroxylation of proline⁵⁶⁴ and proline⁴⁰² in the oxygen dependent degradation domain (ODD) via a reaction that requires 2-oxoglutarate (2OG) and ascorbate.^{4–6} Proline hydroxylation then targets HIF-1 α subunits for proteasomal degradation via binding to the VHL (Von Hippel Lindau tumor suppressor protein), elongin C/B, Cul2, Rbx1 ubiquitin ligase complex. Since the post-translational hydroxylation of HIF-1 α is

controlled by oxygen concentration, under hypoxia the hydroxylation of HIF-1 α is inhibited, and HIF-1 α binds to ARNT to form a functional transcriptional activator that turns on genes with hypoxic response elements (e.g., VEGF, EPO, glycolytic enzymes).⁷ Therefore, inhibition of HIF-1 α prolyl hydroxylases, resulting in HIF-1 α stabilization and has a potential to be a viable therapeutic approach for ischemic diseases including myocardial infarction, stroke, peripheral arterial disease, heart failure, diabetes, and anemia.

Neither crystal structure of the procollagen nor that of HIF prolyl hydroxylases has been reported in the literature. However, atomic resolution structures have been obtained for other 2-oxoglutarate dioxygenases including bacterial proline 3-hydroxylase, deacetoxycephalosporin C synthase, clavaminic synthase, and asparaginyl hydroxylase.⁸ The similarity of cofactor requirements for the catalytic step suggests that these structural data should provide significant information concerning the active site of HIF prolyl hydroxylase to aid synthesis of small molecule inhibitors.

We sought to identify suitable small molecule HIF-1 α prolyl hydroxylase inhibitors based on structure-based design approach utilizing the recently solved crystal structure of EGLN-1⁹ in complex with the isoquinoline inhibitor **1**¹⁰ (Fig. 1).

Keywords: Prolyl hydroxylase inhibitors; HIF1- α ; Hypoxia; Ischemia; Peripheral arterial disease (PAD); Anemia; Pyrazolopyridines.

* Corresponding author. Tel.: +1 513 622 4467; fax: +1 513 622 0523; e-mail: Warshakoon.nc@pg.com

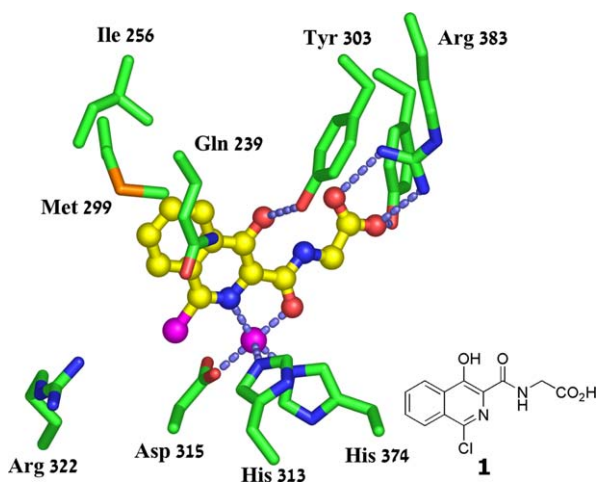


Figure 1. Binding of compound **1** to the catalytic domain of EGLN-1.

Among the key interactions between compound **1** and the EGLN-1 active site are the salt bridge between the terminal carboxylic acid and Arg383, the coordination of iron by the isoquinoline nitrogen and the side chain amide, and also the hydrogen bond between the phenolic hydroxyl of the inhibitor and Tyr303.

In our structure-based drug design approach, pyrazolopyridine **2** emerged as a possible lead for novel HIF-1 α prolyl hydroxylase inhibitors. The predicted binding mode of this compound is shown in Figure 2. In this binding orientation the nitrogens in the pyridine and pyrazole bind to iron, while the carboxylate interacts with Arg383.

The reasonable binding mode of pyrazolopyridine **2** (Fig. 2) prompted us to probe this structural class more carefully. The synthesis of **2** is outlined in the scheme below (Scheme 1).

Additional analogs beginning with **6** were prepared according to the scheme shown below (Scheme 2). The commercially available, 2-chloro-5-hydroxymethylpyridine **6** was protected as its benzyl ether and, in a similar

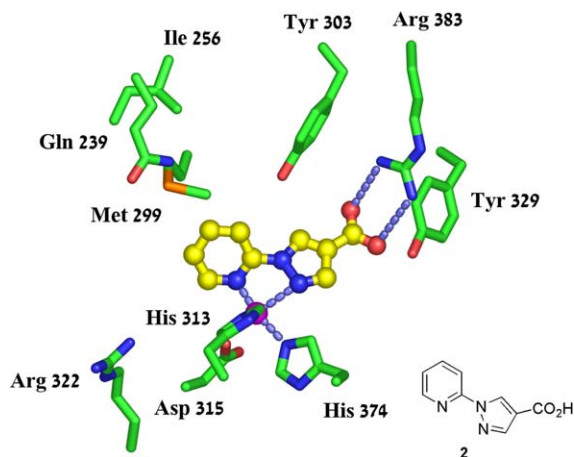


Figure 2. The predicted mode of binding between **2** and EGLN-1.

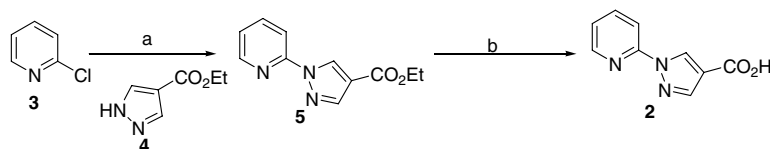
procedure to the synthesis of **2**, was condensed with ethyl pyrazole **4**. However, this reaction did not go to completion, and the separation of the product and the starting material was extremely difficult. Conversely, pyridine *N*-oxide **8** reacted with pyrazole **4** and produced desired condensed product **9** in good yields. Hydrogenation of **9** under microwave conditions cleaved both the benzyl ester and the *N*-oxide. Alkylation of **10** followed by the hydrolysis of the ethyl ester generated the analogs **11a–h** (Table 1).

The benchmark isoquinoline **1** has an IC₅₀ of 1.4 μ M in the EGLN-1 enzyme assay. In comparison, compound **2** showed reasonable activity in the assay (12 μ M) spurring us to initiate a structure-based medicinal chemistry program around the novel pyrazolopyridine scaffold. Figures 2 and 3 show that by reaching out toward the outer region of the active site, ligands can interact favorably with the active site residues Tyr310, Arg322, Met299, and Gln239. The modeling studies suggested that an appropriate substitution placed at the 5-position of the pyridyl nucleus has the ability to interact with these residues, and therefore, brings about the optimal binding energy of the ligands and the active site of EGLN-1.

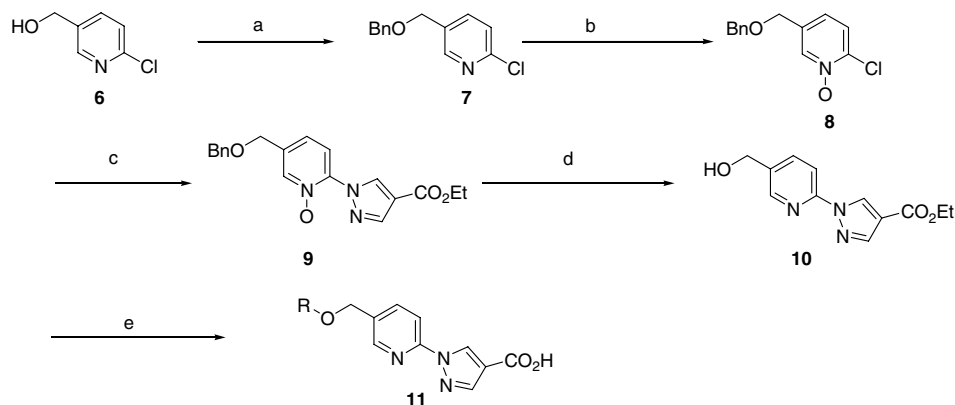
One such analog (compound **11a**) is expected to have a strong coordination to the iron using both the pyridyl and pyrazole nitrogens, while the oxygen atom on the side-chain ether linkage builds a hydrogen bonding interaction with OH of Tyr310. The phenyl ring interacts with the side chain of Gln239 in a lipophilic fashion (Fig. 3).

The pyrazolopyridine analogs were screened in an EGLN-1 enzyme assay (Table 1). The activity of these compounds was then measured in cell-based VEGF induction assay, which measures events downstream of HIF-1 α stabilization (Table 1). In this study, we focused our structure–activity relationship development on the phenyl ring of the distal ether linkage. As suggested by the modeling studies at the outset, the analog **11a** showed good activity against EGLN-1. A range of ring substitutions (both electronic and positional) was tolerated by the enzyme. Thus, both electron-donating and -withdrawing substituents displayed good activity. The *meta*- and *para*-substitutions both showed comparable activity; however, in the case of the chloride substituent, the *para*-substituted pyrazolopyridine **11b** had improved activity as compared to the *ortho*- and *meta*-substitutions (**11c** and **d**). Compound **11i**, in which the distal phenyl ring was substituted with a 2-cyano-phenyl group, had nanomolar activity against the enzyme. In addition to the interactions within the active site, described earlier, we judiciously positioned the nitrile group at the 2-position to build a hydrogen bonding interaction with Trp258 at the top of the active site (Fig. 4). Interestingly, the amide linkage at the 5-position of the pyridyl nucleus had an adverse effect on the activity against EGLN-1 (data not shown).

In the cell-based VEGF assay, these pyrazolopyridines were able to induce significant VEGF induction. In



Scheme 1. Reagents and conditions: (a) $\text{Cs}_2\text{CO}_3/\text{DMF}/140^\circ\text{C}$ (65%); (b) $\text{KOH}/\text{EtOH}/\text{water}$ (90%).



Scheme 2. Reagents and conditions: (a) $\text{BnBr}/\text{THF}/\text{NaH}$ (75%); (b) $\text{MeReO}_3/\text{H}_2\text{O}_2/\text{CH}_2\text{Cl}_2$ (75%); (c) $\text{Cs}_2\text{CO}_3/\text{DMF}/\text{ethylpyrazole-3-carboxylate}/140^\circ\text{C}/30\text{ min}/\text{MW}$ (80%); (d) $\text{Pd}(\text{OH})_2/\text{cyclohexene}/\text{EtOH}/120^\circ\text{C}/20\text{ min}/\text{MW}$ (70%); (e) 1— $\text{RX}/\text{NaH}/\text{THF}$ (65–70%), 2— $\text{KOH}/\text{EtOH}/\text{water}$ (80%).

Table 1. Biological activity of pyrazolopyridines against EGLN-1 and VEGF

Entry	R	EGLN-1- IC_{50} (μM)	VEGF EC_{50} (μM)
11a	H	2.7	25
11b	<i>p</i> -Chloro	0.58	7.4
11c	<i>m</i> -Chloro	1.7	3.8
11d	<i>o</i> -Chloro	2.4	na
11e	<i>p</i> -Methoxy	2.4	1.0
11f	<i>m</i> -Methoxy	1.6	>100
11g	<i>p</i> -Cyano	1.6	na
11h	<i>m</i> -Methyl	2.1	na
11i	<i>m</i> -Trifluoromethyl	2.9	11
11j	<i>p</i> -Isopropyl	1.7	na
11k	3,5-Dimethoxy	2.8	na
11l		0.19	>100

addition, these EGLN inhibitors were effective in stabilizing HIF-1 α . Therefore, this study serves to establish our initial hypothesis of stabilization of HIF-1 α via inhibiting HIF-1 α prolyl hydroxylase and subsequently leading to increase in VEGF induction. Potency changes noted in the enzyme assay were not consistently seen in the cell-based VEGF induction assay. The apparent discrepancies probably reflect the difficulties of reconciling the physical properties of the compounds and

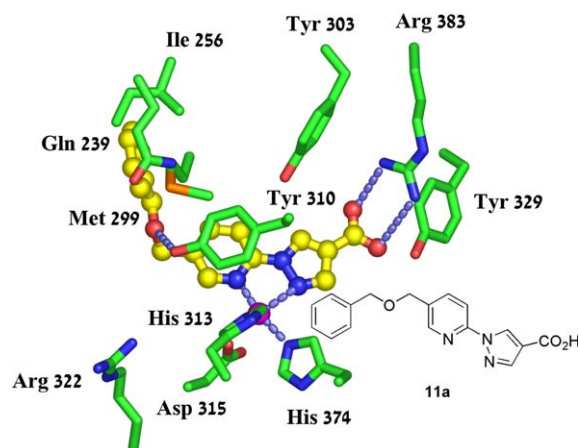


Figure 3. The predicted mode of binding between 11a and EGLN-1.

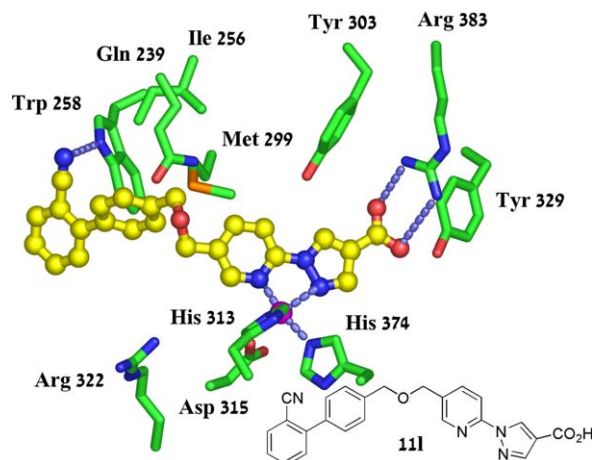


Figure 4. The predicted mode of binding between 11l and EGLN-1.

compatibility with differing conditions and requirements of isolated enzyme and cellular assays.

In summary, this study indicates the ability to design potent, nonpeptidic, HIF-1 α prolyl hydroxylase inhibitors using a structure-based drug design approach. This novel class of pyrazolopyridines is currently under investigation for its PK and in vivo properties. The results will be disclosed elsewhere.

EGLN-1 activity assay. The EGLN-1 enzyme activity was determined using mass spectrometry (matrix-assisted laser desorption ionization, time-of-flight MS, and MALDI-TOF MS). The HIF-1 α peptide corresponding to residues 556–574 (DLDLEALAPYIPADDDDFQL) was used as substrate. The reaction was conducted in a total volume of 50 μ L containing Tris–Cl (5 mM, pH 7.5), ascorbate (120 μ M), 2-oxoglutarate (3.2 μ M), HIF-1 α (8.6 μ M), and bovine serum albumin (0.01%). EGLN-1, quantity predetermined to hydroxylate 20% of substrate in 20 min, was added to start the reaction. Where inhibitors were used, compounds were prepared in dimethylsulfoxide at 10-fold final assay concentration. After 20 min at room temperature, the reaction was stopped by transferring 10 μ L of reaction mixture to 50 μ L of a mass spectrometry matrix solution (α -cyano-4-hydroxycinnamic acid, 5 mg/mL in 50% acetonitrile/0.1% TFA, 5 mM NH_4PO_4). Two microliters of the mixture was spotted onto a MALDI-TOF MS target plate for analysis with an Applied Biosystems (Foster City, CA) 4700 Proteomics Analyzer MALDI-TOF MS equipped with a Nd:YAG laser (355 nm, 3 ns pulse width, 200 Hz repetition rate). Hydroxylated peptide product was identified from substrate by the gain of 16 Da. Data defined as percent conversion of substrate to product were analyzed in GraphPad Prism 4 to calculate IC_{50} values.

VEGF ELISA. HEK293 cells were seeded in 96-well poly-lysine coated plates at 20,000 cells per well in DMEM (10% FBS, 1% NEAA, and 0.1% glutamine). Following overnight incubation, the cells were washed with 100 μ L of Opti-MEM (Gibco, Carlsbad, CA) to remove serum. Compound in DMSO was serially diluted (beginning with 100 μ M) in Opti-MEM and added to

the cells. The conditioned media were analyzed for VEGF with a Quantikine human VEGF immunoassay kit (R&D Systems, Minneapolis, MN). Optical density measurements at 450 nm were recorded using the Spectra Max 250 (Molecular Devices, Sunnyvale, CA). Data defined as % of DFO stimulation were used to calculate EC_{50} values with GraphPad Prism 4 software.

Acknowledgments

NCW wishes to thank Dr. Joseph Gardner for his continuous support and guidance. Ms. Anne Russell and Ms. Marcia Ketcha are gratefully acknowledged for analytical instrumentation support. The authors wish to acknowledge Chuiying Li for EGLN-1 cloning studies and Michelle Tscheiner for the synthesis of HIF-1 α peptide.

References and notes

1. Mack, C. A.; Magovern, C. J.; Budenbender, K. T.; Patel, S. R.; Schwatz, E. A.; Zanzonico, P.; Ferris, B.; Sanborn, T.; Isom, O. W.; Crystal, R. G.; Rosengart, T. K. *J. Vasc. Surg.* **1998**, *27*, 699.
2. Bruick, R. K.; McKnight, S. L. *Genes Dev.* **2001**, *15*, 2497.
3. Safran, M.; Kaelin, W. G., Jr. *J. Clin. Invest.* **2003**, *111*, 779.
4. Semenza, G. L. *J. Appl. Physiol.* **2000**, *88*, 1474.
5. Semenza, G. L. *Cell* **2001**, *107*, 1.
6. Kondo, K.; Kaelin, W. G., Jr. *Exp. Cell Res.* **2001**, *264*, 117.
7. Semenza, G. *Biochem. Pharmacol.* **2002**, *64*, 993.
8. (a) Cunliffe, C. J.; Franklin, T. J.; Hales, N. J.; Hill, G. B. *J. Med. Chem.* **1992**, *35*, 2652; (b) Valegard, K.; Van Scheltinga, A. C.; Lloyd, M. D.; Hara, T.; Ramaswamy, S.; Parrakis, A.; Thompson, A.; Lee, H. J.; Baldwin, J. E.; Schofield, C. J.; Hajdu, J.; Anderson, I. *Nature* **1998**, *394*, 805; (c) Zhang, Z.; Ren, J.; Harlos, K.; McKinnon, C. H.; Clifton, I. J.; Schofield, C. J. *FEBS Lett.* **2002**, *517*, 7; (d) Elkins, J. M.; Hewitson, K. S.; McNeill, L. A.; Seibel, J. F.; Schlemminger, I.; Pugh, C. W.; Ratcliffe, P. J.; Schofield, C. J. *J. Biol. Chem.* **2003**, *278*, 1802.
9. Evdokimov, et al., *Nat. Struct. Mol. Biol.* **2006**, under review.
10. Guenzler, P.; Volkmar, K.; Stephen, J.; Liu, D. Y.; Todd, W. PCT. In. Appl. WO 2005007192, **2005**.